Journal of Inclusion Phenomena and Macrocyclic Chemistry **36:** 217–228, 2000.

Hydrates of Thiothixene·2HCl: Kinetics of Dehydration and Crystal Structure of the Methanol Solvate

SUSAN A. BOURNE*, ANITA COETZEE and AYESHA JACOBS
Department of Chemistry, University of Cape Town, Rondebosch 7701, South Africa

(Received: 30 October 1998; in final form: 28 January 1999)

Abstract. Thiothixene·2HCl forms three different hydrates on exposure to water vapour. These have been characterised by X-ray powder diffraction. The dehydration reaction of the monohydrate follows the first-order rate law with E_a = 125(22) kJ mol^{-1}. The dehydration of the tetrahydrate follows a complex mechanism. The crystal structure of the methanol solvate of thiothixene·2HCl has been elucidated. It is monoclinic, P2$_1$/c, a = 18.870, b = 7.018, c = 21.913 Å, β = 105.622°.

Key words: inclusion compounds, Thiothixene 2HCl, kinetics of dehydration

Supplementary Data relating to this article (bond lengths and angles, tables of observed and calculated F) are deposited with the British Library as Supplementary Publication No. SUP 82260 (15 pages)

1. Introduction

Drug hydrates are formed when water is entrapped in the respective crystal structures. Hydrates can be classified into two broad classes [1]:

(a) Polymorphic hydrates rearrange to another crystal form on desolvation.
(b) Pseudopolymorphic hydrates remain in the same crystal form upon desolvation, if the water molecules occupy voids in the crystal structure and no interactions with the drug are present, desolvation does not destroy the crystal structure.

The drug thiothixene·2HCl (**1**) is used in psychotherapy and is particularly effective in treating schizophrenia. The FDA water specification for this drug is 6.2–7.5% (by weight). This corresponds to the dihydrate, **1**·2H$_2$O which is very labile and water absorption and desorption occurs rapidly depending on conditions of temperature and relative humidity. Different hydrates can be formed which makes storage and transport of **1** difficult. Thus understanding the absorption/desorption processes and hydrate stabilities would be of value in optimizing storage conditions.

* Author for correspondence.

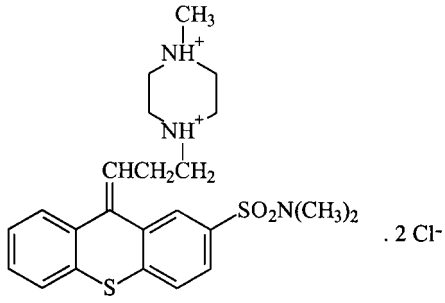

Scheme 1. **1.**

In this article, we report the formation of three different hydrates of **1** and the kinetics of dehydration of the monohydrate form. The crystal structure of the inclusion compound of **1** with methanol (**2**) is also reported here.

2. Experimental

1·2H_2O was supplied by Fine Chemicals Corp (Cape Town). The monohydrate (**1**·H_2O) was obtained by drying the dihydrate sample supplied under vacuum in a Buchi TO-51 drying oven for two hours at 105 °C.

2.1. THERMAL ANALYSIS

The stoichiometry of the different hydrates was established using thermogravimetry (TG). This was performed on a Perkin Elmer Series 7 instrument. Samples of 3–7 mg were heated in an open platinum pan under a constant flow of dry nitrogen (40 cm^3 min^{-1}). All samples were sieved and the fraction with particle size 90–150 μm was used. Programmed temperature runs were carried out at 10 °C min^{-1} over a temperature range 30–200 °C.

To determine the activation energy of the dehydration reaction of **1**·H_2O, isothermal TG was used, as previously described [2]. TG runs were performed at 2–3 °C intervals in the range 32–45 °C. The resulting mass loss vs time curves were converted into α (extent of reaction) vs time curves. A number of kinetic models of the form $f(\alpha) = kt$ were fitted to the data and the model chosen which was most linear over the widest α range. The rate constant k was obtained for each temperature in the range and an Arrhenius type plot ($\ln k$ vs $1/T$) was then used to determine the activation energy of the dehydration reaction.

2.2. CRYSTAL STRUCTURE DETERMINATION

Rod-like crystals of **2** were obtained by slow cooling of a solution of **1** in methanol. A suitable single crystal was mounted in mother liquor in a capillary tube to prevent desolvation during data collection. Intensity X-ray data were collected on a Nonius

Table I. Thermogravimetry results for hydrates of **1**

Compound	Calculated mass loss (%)	Observed mass loss (%)
1·H_2O	3.37	3.42
1·2 H_2O	6.52	6.65
1·4 H_2O	12.24	12.61

Kappa CCD diffractometer with graphite-monochromated Mo Kα radiation (λ = 0.7107 Å) at 20 °C. Data were collected over a 180° rotation in ϕ using a step size of 1° and a scan time of 40 s per frame. Dezingering was accomplished by collecting each frame twice and averaging. The data was processed using DENZO-SMN [3].

The crystal structure was solved by direct methods using SHELXS86 [4] and refined by least squares on F^2 using SHELXL93 [5]. All non-hydrogen atoms were refined anisotropically while the hydrogens on the thiothixene molecule were placed in calculated positions with a common temperature factor. Hydrogens on the nitrogen atoms and those of the methanol guest were not included in the final model.

2.3. X-RAY POWDER DIFFRACTION (XRD)

XRD was done on a Philips PW1130/90 X-ray diffractometer using Co Kα radiation (λ = 1.7902 Å). The samples were scanned at $6° \leq 2\theta \leq 40°$ with a step size of 0.1° and a counting time of 2 s. The calculated XRD pattern for the crystal structure was produced using LAZY-PULVERIX [6].

3. Results and Discussion

Under different conditions, several hydrates of **1** were found to form. TG (Table I) and XRD (Figure 1) were used to characterize the monohydrate, dihydrate and the tetrahydrate. Anhydrous **1** could not be isolated.

3.1. ABSORPTION OF WATER BY **1**

In an attempt to determine the reaction pathway followed during the absorption of water by **1**, the monohydrate, **1**·H_2O, was exposed to water vapour over an extended time period. The material was sampled for TG at times from 30 minutes up to 30 days. An identical sample of the monohydrate was placed in an aluminium sample pan in the XRD goniometer along with a vial filled with water. This sample was scanned at $9° \leq 2\theta \leq 20°$ with a step size of 0.05° and a time constant of 1 second. One complete scan took approximately 10 minutes. Consecutive scans

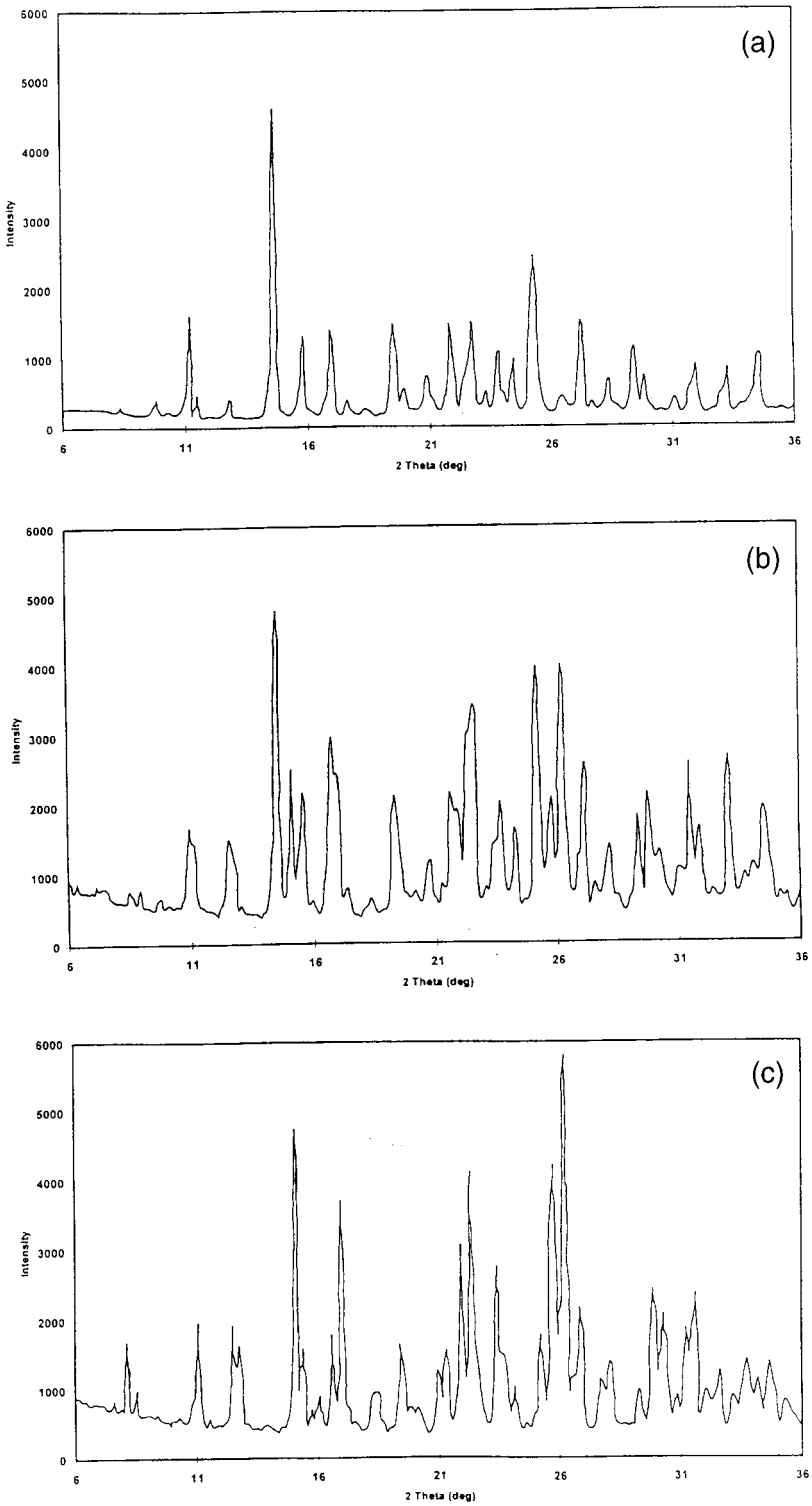

Figure 1. XRD patterns of (a) **1**·H_2O, (b) **1**·$2H_2O$, (c) **1**·$4H_2O$.

Table II. Comparison of kinetic models for the dehydration of **1**·H_2O

Model	$f(\alpha) = kt$	Region of linearity	Correlation coefficient
First order (F1)	$-\ln(1-\alpha)$	0.3–1.0	0.98–0.99
Contracting area (R2)	$1-(1-\alpha)^{1/2}$	0.5–0.8	0.90
Contracting sphere (R3)	$1-(1-\alpha)^{1/3}$	0.3–0.8	0.92–0.95

were collected for four hours. Both of these experiments showed the formation first of the dihydrate (within ca 30 minutes). Within 2 hours, the tetrahydrate had been formed, and there was no further change. Thus the following general reaction pathway can be suggested for the absorption process:

$$\mathbf{1}\cdot H_2O \rightarrow \mathbf{1}\cdot 2H_2O \rightarrow \mathbf{1}\cdot 4H_2O.$$

3.2. DESORPTION OF WATER FROM **1**·H_2O

$$\mathbf{1}\cdot H_2O(s) \rightarrow \mathbf{1}\ (s) + H_2O\ (g).$$

Isothermal TG was performed at 2–3 °C intervals over a temperature range of 32 to 45 °C. On conversion to α-time curves, the reaction was seen to be deceleratory. A number of different models were fitted to the data. The best fitting models are listed in Table II. The reaction mechanism that best fitted the data was the first-order rate expression, F1 ($f(\alpha) = -\ln(1-\alpha)$) with a correlation coefficient r = 0.98–0.99 over the temperature range. The fact that the data fitted one kinetic model indicated that the decomposition of the monohydrate is isokinetic, i.e., the activation energy is independent of the extent of the reaction and of temperature. Hence the Arrhenius equation can be used to determine the activation energy. Figure 2 shows the appropriate Arrhenius plot for this reaction. The activation energy obtained was 125(22) kJ mol^{-1} (ln A = 44.5(3)). This value is comparable with activation energies obtained for organic inclusion compounds which usually range from 30 to 200 kJ mol^{-1} [7].

3.3. DESORPTION OF WATER FROM **1**·$4H_2O$

Although the desorption of water from **1**·$4H_2O$ appears in the programmed temperature TG to be a single step process, attempts to determine the activation energy by the isothermal method described above failed. The method developed by Flynn and Wall [8] for the decomposition of polymers has been successfully applied to certain inclusion compounds [9] so we attempted to apply this method to the dehydration reaction of **1**·$4H_2O$.

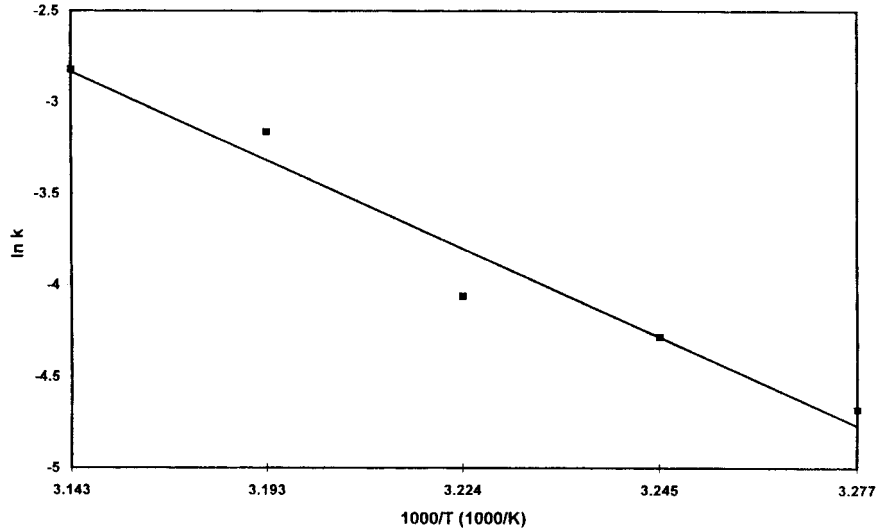

Figure 2. Arrhenius plot for the dehydration of **1**·4H_2O.

The thermogravimetric rate is

$$\frac{d\alpha}{dT} = \frac{A}{\beta} f(\alpha) e^{-E/RT}$$

which can be simplified to

$$\frac{d \log \beta}{d\frac{1}{T}} \cong \frac{0.457}{R} E$$

where E is the activation energy and β is the heating rate in °C min^{-1}.

TG of **1**·4H_2O was performed at different heating rates from 2.5 °C min^{-1} to 20 °C min^{-1}. For each TG curve the corresponding temperatures at a constant mass loss were determined. Plots of $-\log \beta$ vs $1/T$ were made for each constant mass loss and the activation energy obtained from the slopes of these graphs. The results obtained are shown in Figure 3 and in Table III. These plots are non-isokinetic, i.e., the activation energy depends on the extent of reaction. In particular, E_a appears to be higher at low heating rates. The activation energies obtained range between 24 and 164 kJ mol^{-1}. We propose that this decomposition is in fact a multiple step process, as shown below:

$$\mathbf{1}\cdot 4H_2O \rightarrow \mathbf{1}\cdot 2H_2O \rightarrow \mathbf{1}\cdot H_2O \rightarrow \mathbf{1}$$

The instability of the dihydrate, **1**·2H_2O prevented a study of its rate of dehydration.

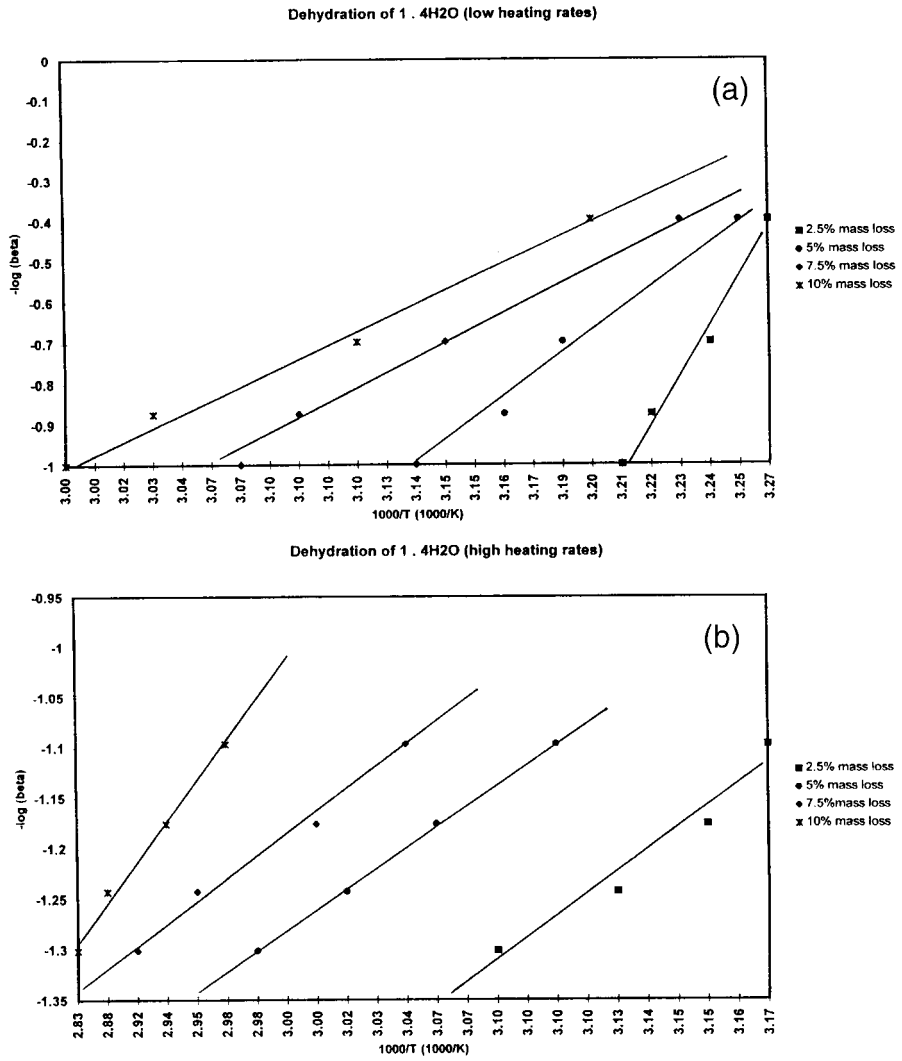

Figure 3. Kinetic plots for the dehydration of **1**·4H_2O: (a) Heating rates 2.5–10 °C min^{-1}. (b) Heating rates 12.5–20 °C min^{-1}.

3.4. CRYSTAL STRUCTURE OF **2**

Crystals of the hydrates of **1** suitable for single crystal studies could not be obtained. However we have elucidated the structure of **1** with methanol. (**2**: **1**·CH_3OH). Both thiothixene·2HCl and methanol were located in general positions. Figure 4 shows the molecular structure and the atomic labelling scheme used. Details of crystal data collection and structure refinement are given in Table IV. Atomic coordinates are listed in Table V. Bond lengths and angles fell within expected ranges [10].

Table III. Kinetic data for the dehydration of **1**· $4H_2O$

Mass loss (%)	Slope of curve	Activation energy (kJ mol^{-1})
Heating rates: 2.5, 5, 7.5 and 10 °C min^{-1}		
10	2980.8	54.2
7.5	3905.1	71.0
5.0	5227.7	95.1
2.5	8991.4	163.6
Heating rates: 12.5, 15, 17.5 and 20 °C min^{-1}		
10.0	1366	24.9
7.5	1573.2	28.6
5.0	1663.5	30.3
2.5	2755.5	50.1

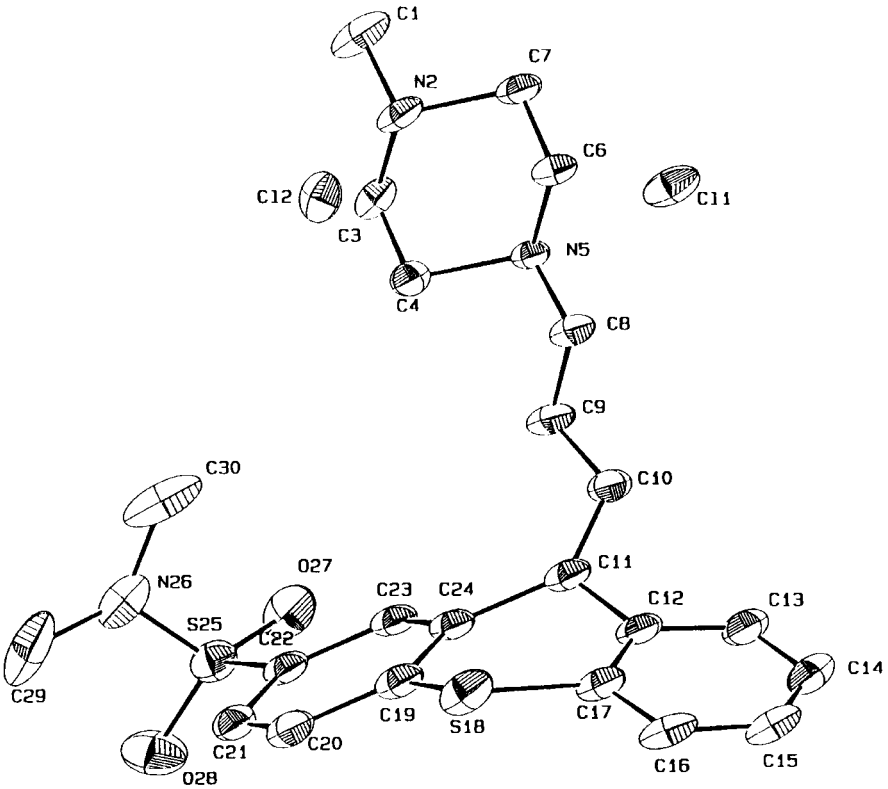

Figure 4. Molecular structure of **2**. Hydrogens omitted for clarity. Other atoms are shown with ellipsoids of 30% probability.

Table IV. Crystal data and structure refinement parameters for **2**

Molecular formula	$(C_{23}H_{31}N_3O_2S_2)^{2+}\cdot Cl_2^{2-}\cdot CH_3OH$
Formula weight	548.57
Temperature (K)	293(2)
Crystal system	Monoclinic
Space group	$P2_1/c$
a (Å)	18.870(2)
b (Å)	7.018(2)
c (Å)	21.913(2)
β (°)	105.622(2)
Volume (Å^3)	2794.7(9)
Z	4
Density (calculated) (g cm^{-3})	1.304
Absorption coefficient (mm^{-1})	0.411
$F(000)$	1160
Crystal size (mm)	0.25 × 0.30 × 0.30
Theta range for data collection (°)	3.06–31.31
Index ranges	$-25 \le h \le 24$; $-7 \le k \le 0$; $0 \le l \le 21$
Reflections collected	5121
Independent reflections	5121
Refinement method	Full matrix least-squares on F^2
Data/restraints/parameters	5121/0/305
Goodness of fit on F^2	1.072
Final R indices ($I > 2\sigma I$)	$R1 = 0.0830$, $wR2 = 0.2339$
R indices (all data)	$R1 = 0.1221$, $wR2 = 0.2570$
Largest diff. peak and hole (e Å^{-3})	0.962 and −1.290 (vicinity of guest)

Least-squares planes through the aromatic rings (C(12)–C(17) and C(19)–C(24)) show little deviation from planarity (r.m.s. deviation <0.013 Å). The angle between the two rings is 34.0(2)°. This gives rise to the bowed shape of the aromatic region of this molecule. The piperazinyl ring is in the chair conformation, with N(2) and N(5) above and below the plane by 0.68 Å.

No interactions between thiothixene and methanol are apparent. It appears that the methanol guest fits into voids created by the packing of the host molecules. The fact that there are no interactions may explain the lability of the methanol solvate.

The crystal packing is shown in Figure 5. Thiothixene molecules pack with complementary bowed regions in a bilayer parallel to [001]. The piperazinylpropyl moiety acts as a spacer between the bilayers allowing for the inclusion of methanol molecules. There is a chloride associated with each piperazinyl nitrogen atom,

Table V. Atomic coordinates ($\times 10^4$) and equivalent isotropic displacement parameters ($Å^2 \times 10^3$) for **2**. $U(eq)$ is defined as one third of the trace of the orthogonalized Uij tensor

	x	y	z	$U(eq)$
C(1)	5586(2)	7114(7)	6142(3)	82(2)
N(2)	4977(2)	7990(5)	6200(2)	53(1)
C(3)	4435(2)	7362(7)	5585(2)	56(1)
C(4)	3830(2)	8358(7)	5630(2)	52(1)
N(5)	3689(1)	7895(4)	6346(2)	39(1)
C(6)	4244(2)	8520(6)	6964(2)	48(1)
C(7)	4847(2)	7524(6)	6912(2)	53(1)
C(8)	3091(2)	8798(6)	6435(2)	48(1)
C(9)	2505(2)	8282(7)	5833(2)	56(1)
C(10)	1927(2)	8990(6)	6020(2)	53(1)
C(11)	1459(2)	10092(6)	5613(2)	50(1)
C(12)	941(2)	10756(6)	5928(2)	54(1)
C(13)	652(2)	9528(8)	6324(3)	65(1)
C(14)	196(2)	10207(9)	6636(3)	75(2)
C(15)	6(2)	12084(9)	6556(3)	77(2)
C(16)	264(2)	13290(8)	6144(3)	70(2)
C(17)	727(2)	12630(7)	5827(2)	57(1)
S(18)	1059(1)	14250(2)	5314(1)	72(1)
C(19)	1236(2)	12681(6)	4674(3)	58(1)
C(20)	1197(2)	13372(7)	3970(3)	64(1)
C(21)	1332(2)	12200(7)	3446(3)	62(1)
C(22)	1513(2)	10326(6)	3627(2)	53(1)
C(23)	1552(2)	9623(6)	4324(2)	51(1)
C(24)	1425(2)	10790(6)	4863(2)	50(1)
S(25)	1676(1)	8822(2)	2951(1)	61(1)
N(26)	2335(3)	9515(8)	2806(3)	82(1)
O(27)	1760(2)	6943(5)	3247(2)	82(1)
O(28)	1202(2)	9178(6)	2285(2)	95(1)
C(29)	2311(4)	11355(11)	2404(5)	127(3)
C(30)	2916(3)	9150(12)	3383(5)	128(3)
Cl(1)	3664(1)	1293(2)	1667(1)	67(1)
Cl(2)	4760(1)	7886(2)	3834(1)	60(1)
OG1	3472(5)	1803(11)	−6(4)	163(3)
CG1	2850(6)	1283(13)	−341(5)	129(3)

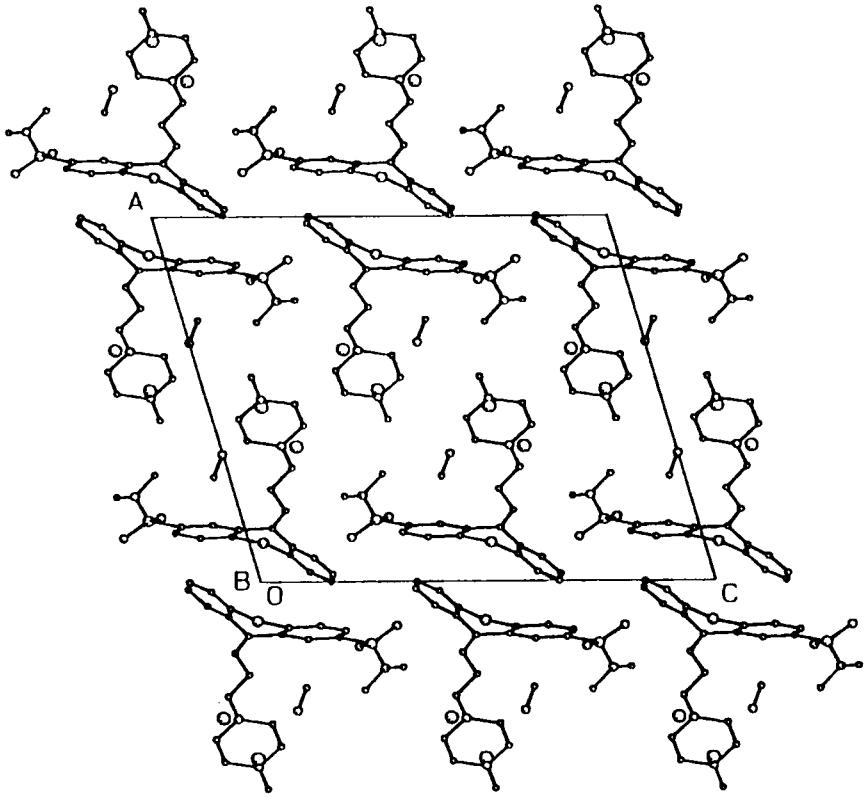

Figure 5. Crystal packing in **2** viewed along [010].

with nitrogen to chloride distances of 2.940(4) Å (N(2)···Cl(2)) and 3.025(3) Å (N(5)···Cl(1)).

2 was too unstable in air to allow its XRD pattern to be measured. However, we are able to calculate the XRD pattern using the atomic coordinates determined in the single crystal structure. This is shown in Figure 6. It shows significant differences in *d*-spacing and relative intensity to any of the hydrates of **1** that we have measured. Thus we conclude that the crystal structure of the hydrates are all quite different to that of the methanol solvate, **2**.

4. Conclusion

Three hydrates of **1** have been shown to form. Of these, the dihydrate is the least stable. Conversion from one hydrate to the others is easily achieved. Thus the transport and storage of this material may be accomplished using any hydrate which can then be converted to the desired material just before use.

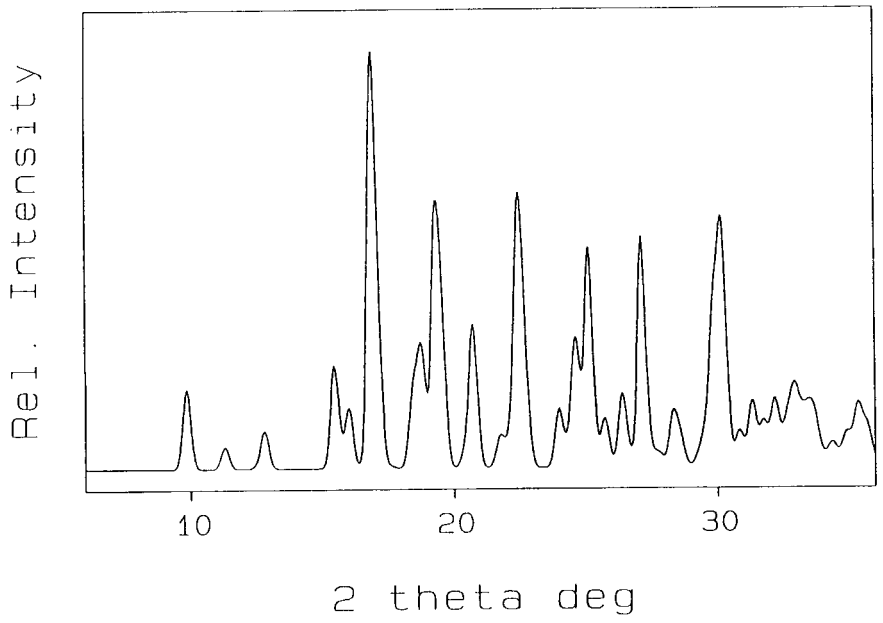

Figure 6. Calculated XRD pattern of **2**.

Acknowledgements

The authors thank the Foundation for Research Development and the University of Cape Town for financial assistance and Fine Chemicals Corp for supplying the thiothixene·2HCl.

References

1. S. R. Byrn: *Solid State Chemistry of Drugs*, Academic Press, New York (1982).
2. M. R. Caira, A. Coetzee, L. R. Nassimbeni, E. Weber, and A. Wierig: *J. Chem. Soc., Perkin Trans. 2* 237, (1997).
3. Z. Otwinowski and W. Minor: in C. W. Carter, J. Sweet, and R. M Sweet (eds.), *Processing of X-ray Diffraction Data Collected in Oscillation Mode, Methods in Enzimology: Macromolecular Crystallography, Part A*, Vol. 276, Academic Press, New York, (1997), p. 307.
4. G. M. Sheldrick: *Acta Crystallogr.* **A46**, 467 (1990).
5. G. M. Sheldrick: SHELXL93, unpublished.
6. K. Yvon, W. Jeitschko, and E. Parthe: *J. Appl. Crystallogr.* **10**, 73 (1977).
7. K. L. Gifford Nash: Ph.D. thesis, University of Cape Town (1997).
8. J. H. Flynn and L. A. Wall: *Polymer Letters* **4**, 323 (1966).
9. M. R. Caira, A. Horne, L. R. Nassimbeni, and F. Toda: *J. Mater. Chem*. **7**, 2145 (1997).
10. F. H. Allen, O. Kennard, D. G. Watson, L. Brammer, A. G. Orpen, and R. Taylor: *J. Chem. Soc., Perkin Trans. 2* S1 (1987).